# Fast trajectory planning by design of initial trajectory in overhead traveling crane with considering obstacle avoidance and load vibration suppression

**Akira Inomata, Yoshiyuki Noda**

Department of Mechanical Systems Engineering, University of Yamanashi, 4-3-11, Takeda, Kofu, Yamanashi, Japan

E-mail: g15mm006@yamanashi.ac.jp

**Abstract.** This paper is concerned with an advanced transfer trajectory planning method of 2-Dimensional transfer machine with vibrational element such as an overhead traveling crane. In the 2-D transfer machine, it is required to reach the target position in a short time, avoid the obstacles, and suppress the vibration. In recent years, the authors have proposed the trajectory planning method using the optimization problem with considering input and state constraints in the transfer system, obstacle avoidance and vibration suppression. However in the previous approaches, it takes a long time to derive the reference trajectory because of many variables in the optimization. Therefore in this study, we propose the fast solution for optimizing the transfer trajectory by giving a feasible initial trajectory. And, it is discussed how to give the cost function in the trajectory optimization with reducing the fluctuating cart motion. Moreover, we discuss the practical case that the proposed approach is applied to the large transfer space. The effectiveness of the proposed transfer trajectory planning method is verified by simulations of the overhead traveling crane.

## 1. Introduction

In many industries, overhead traveling crane systems frequently have been used for efficiently transporting heavy loads. In the overhead traveling crane, it is required to reach the target position in a short time, avoid the obstacles, and suppress sway of the load [1]∼[4].

In order to fulfill the above requirements, the transfer control systems have been proposed in the previous studies. The vibration suppression control to load of the overhead crane using optimal control theory was proposed in [5]. In the crane system with varying the rope length, the load vibration with varying the natural frequency is suppressed by the gain scheduling control [6], [7]. Furthermore, natural frequency elements of vibration are eliminated by shaping the acceleration of the cart [8]. These control systems have specialized in the load sway suppression. In the 2-D transfer systems such as the overhead traveling crane, a path planning considering obstacle avoidance is required. In the studies of path planning, the path of transferred object has been derived by the potential method [9], the probabilistic road map method [10], and predicting the action of the moving obstacle [11]. In the study [12], the path in consideration of obstacles avoidance is derived by the potential method. Then, the path is reshaped to the trajectory

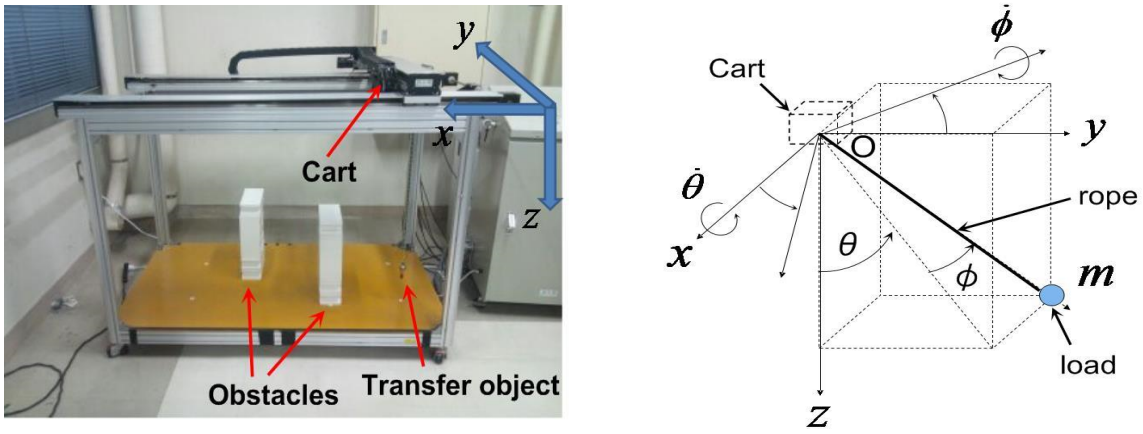


(a) Photo of laboratory-type overhead traveling crane

(b) Illustration of load sway in crane

**Figure 1.** Overhead traveling crane system

with vibration suppression. In this approach, the reshaped trajectory is different from the path for avoiding the obstacle derived by the potential method. Therefore, the transfer object is in danger of collision with obstacles.

In recent years, the trajectory planning methods in consideration of input and state constraints in the transfer system, suppressing the load sway with varying the rope length, and the obstacles avoidance in the transfer space have been proposed by authors [13], [14]. In these approaches, the trajectory planning problem is formulated as the quadratic problem with quadratic constraints in the optimization problem. Thus, the trajectory is optimized by a sequential quadratic programming approach.

However in the previous approaches, it takes a long time to derive the reference trajectory because of many variables in the optimization. Therefore in this study, we propose the fast solution for optimizing the transfer trajectory by giving a feasible initial trajectory to the trajectory optimization. And, it is discussed how to give the cost function in the trajectory optimization with reducing the fluctuating cart motion. Moreover, we discuss the practical case that the proposed approach is applied to the large transfer space. The effectiveness of the proposed transfer trajectory planning method is verified by simulations of the overhead traveling crane.

## 2. Model of overhead traveling crane system

In this study, the proposed control system is applied to the overhead traveling crane system as one of the 2-D transfer system with vibrational element. The overhead traveling crane used in this study is shown in Figure 1(a). And, schematic illustration of the load sway is shown in Figure 1(b). Specifications of the overhead traveling crane in Figure 1(a) are shown in Table 1. The model of load sway dynamics is linearized as $\theta \ll 1$, $\phi \ll 1$, and it is represented as

$$\begin{cases} ml^2\ddot{\theta} + mgl\theta = mla_y, \\ ml^2\ddot{\phi} + mgl\phi = -mla_x, \end{cases} \tag{1}$$

where $m$ is mass of the load, $g$ is a gravity acceleration, $l$ is the rope length, and $\theta$ and $\phi$ are the load sway angles, $a_x$ and $a_y$ are acceleration of the cart transfer of each axis. The cart transfer system consists of the position feedback control system. The feedback controllers on $x$- and $y$-axes have the proportional gain. The cart transfer systems on $x$- and $y$-axes are represented as

**Table 1.** Specifications of crane system shown in Figure 1(a)

| | |
|---|---|
| Maximum Transfer Distance on $x$-axis | 1.050[m] |
| Maximum Transfer Distance on $y$-axis | 0.400[m] |
| Maximum Rope Length | 0.60[m] |
| Limitations of Velocities on $x$-and $y$-axes | ± 0.22[m/s] |
| Limitations of Hoisting Velocity | ± 0.5[m/s] |
| Limitations of Accelerations on $x$- and $y$-axes | ± 0.5[m/s$^2$] |
| Limitations of Hoisting Acceleration | ± 1.0[m/s$^2$] |
| Limitation of Control Input Voltage | ± 10[V] |

$$\begin{cases} \ddot{x}_{cm} = -\frac{1}{T_m}\dot{x}_{cm} + \frac{K_m}{T_m}u_m, \\ u_m = K_{pm}(r_m - x_{cm}), \qquad\qquad (m = x, y), \end{cases} \tag{2}$$

where $x_{cm}$, $u_m$ and $r_m$ are the cart position, the control input, and the reference trajectory of each axis, respectively. $T_m$ and $K_m$ are the time constant and the gain in the motor of each axis, respectively. $K_{pm}$ is the proportional gain in the position feedback controller of each axis. In this study, the time constant and the gain in each motor can be obtained as $T_x$=0.008[s], $T_y$=0.036[s] and $K_x$=$K_y$=0.037[m/s/V] by the parameter identification, respectively. The proportional gains are given as $K_{px}$=$K_{py}$=100.

## 3. Transfer trajectory planning method

The transfer trajectory planning method using optimization method has been proposed in the author's studies [13], [14]. The detailed derivation of the method is referred to in [13], [14].

### *3.1. Representation of controlled object*

In this study, the cart motion with input and state constraints as shown in Figure 2 can be controlled according to the trajectory planning. Therefore, the cart motion as the controlled object is represented as

$$\begin{cases} x_m(k+1) = A_{clm}x_{dm}(k) + B_{clm}r_m(k), \\ z_m(k) = C_{zclm}x_{dm}(k) + D_{zclm}r_m(k), \\ z_{um}(k) = C_{uclm}x_{dm}(k) + D_{uclm}r_m(k), \\ y_m(k) = C_{yclm}x_{dm}(k) + D_{yclm}r_m(k), \quad (m = x, y), \end{cases} \tag{3}$$

where $x_{dm}$ is the state variable vector, $z_m$ is the controlled variable vector. The vector $z_m$ consists of the cart position, velocity and acceleration, $z_{um}$ is the control input, $y_m$ is the cart position as the observed variable.

In order to formulate the trajectory planning to optimization problem, the cart motion is represented with the discrete-time system as $t = k\Delta T$. Here, $t$ is the time, $\Delta T$ is the sampling time and $k$ is the sample number. As shown in Figure 2, the control input $z_{um}$ and the controlled variables $z_m$ are subject to the input and state constraints.

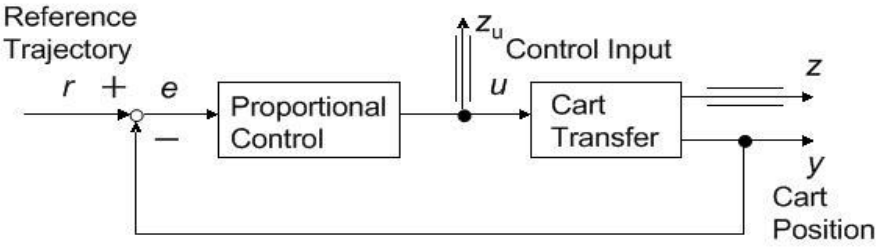


**Figure 2.** Cart transfer system as controlled object on an axis

*3.2. Cost function*

The cost function is defined for the transfer trajectory optimization. The transfer trajectory derived by the previous approaches [13], [14] has the fluctuating motion. Because, the energy saving is not considered in the cost function. In order to reduce the fluctuating motion, the cost function with energy saving is proposed as

$$\begin{aligned}\min_{r_x,r_y} J &= w_1\Big(\sum_{k=0}^{N-1} \mid r_{0x}(k)-x(k) \mid^2 + \sum_{k=0}^{N-1} \mid r_{0y}(k)-y(k) \mid^2\Big) \\ &+ w_2\Big(\sum_{k=0}^{N-1} \mid z_{ux}(k) \mid^2 + \sum_{k=0}^{N-1} \mid z_{uy}(k) \mid^2\Big) \\ &+ w_3\Big(\int_{v_1}^{v_2} \mid z_{ux}(v) \mid^2 dv + \int_{v_1}^{v_2} \mid z_{uy}(v) \mid^2 dv\Big), \end{aligned} \tag{4}$$

where $r_{0x}$ and $r_{0y}$ are the target positions on $x$- and $y$ - axes, respectively. $v$ is the frequency. $v_1$ and $v_2$ are the minimum and maximum frequencies. And, $w_1 \geq 0$, $w_2 \geq 0$ and $w_3 \geq 0$ are the weight coefficients.

Here, the vectors of the input and controlled variables are respectively defined as

$$\begin{aligned} Z_{um} &= [z_{um}(0) \quad z_{um}(1) \quad \cdots z_{um}(N-1)]^T, \\ Z_m &= [z_m(0) \quad z_m(1) \quad \cdots z_m(N-1)]^T, \quad (m=x,y). \end{aligned} \tag{5}$$

We also define vectors $R_m$, $R_{0m}$ and $Y_m$ $(m = x, y)$ whose elements are $r_m(k)$, $r_{0m}(k)$ and $y_m(k)$, $(k = 0, 1, \cdots, n-1)$, respectively. Therefore, the control input and the controlled and observation variables can be compactly expressed as

$$Z_m = M_{zm}R_m, \quad Y_m = M_{ym}R_m, \quad (m=x,y), \tag{6}$$

where $M_{zm}$ and $M_{ym}$ are given by

$$M_{zm} = \begin{bmatrix} D_{zclm} & 0 & \cdots & 0 \\ C_{zclm}B_{clm} & D_{zclm} & \cdots & \vdots \\ \vdots & \vdots & \ddots & 0 \\ C_{yclm}A_{clm}^{n-2} & \cdots & C_{zclm}B_{clm} & D_{zclm} \end{bmatrix}, \tag{7}$$

$$M_{ym} = \begin{bmatrix} D_{yclm} & 0 & \cdots & 0 \\ C_{yclm}B_{clm} & D_{yclm} & \cdots & \vdots \\ \vdots & \vdots & \ddots & 0 \\ C_{yclm}A_{clm}^{n-2} & \cdots & C_{yclm}B_{clm} & D_{yclm} \end{bmatrix}, \quad (m=x,y). \tag{8}$$

Excluding the weight coefficient $w_1$, the first term $J_1$ and second term $J_2$ in the cost function (4) becomes

$$J_{12} = (R_x^T M_{yx}^T M_{yx} R_x - 2R_x^T M_{yx}^T R_{0x}) + (R_y^T M_{yy}^T M_{yy} R_y - 2R_y^T M_{yy}^T R_{0y}), \tag{9}$$

where since $R_{0x}^T R_{0x}$ and $R_{0y}^T R_{0y}$ are constants, they have been omitted from the cost function. We also express the third term $J_3$ and fourth term $J_4$ in the cost function (4) without the weight coefficient $w_2$ to the matrix representation as

$$J_{34} = (R_x^T M_{zux}^T M_{zux} R_x) + (R_y^T M_{zuy}^T M_{zuy} R_y). \tag{10}$$

Excluding the weight coefficient $w_3$, the fifth term $J_5$ in the cost function (4) can be discrete Fourier transformed as

$$\begin{aligned} J_5 = \int_{v_1}^{v_2} \mid z_{ux}(v) \mid^2 dv &= \int_{v_1}^{v_2} \mid \sum_{k=0}^{N-1} z_{ux}(k) e^{-jv\Delta Tk} \mid^2 dv \\ &= \int_{v_1}^{v_2} \sum_{k=0}^{N-1} z_{ux}(k) e^{-jv\Delta Tk} * \sum_{k=0}^{N-1} e^{jv\Delta Tk} z_{ux}(k) dv. \end{aligned} \tag{11}$$

The sixth term $J_6$ in the cost function (4) can be represented similarly to $J_5$. Therefore, the matrix representation of fifth term $J_5$ and sixth term $J_6$ in the cost function (4) can be expressed as

$$J_{56} = R_x^T M_{zux}^T \overline{M}_e M_{zux} R_x + R_y^T M_{zuy}^T \overline{M}_e M_{zuy} R_y, \tag{12}$$

where $\overline{M}_e$ is given by

$$\overline{M}_e = \begin{bmatrix} v_2 - v_1 & \frac{\sin v_2\Delta T - \sin v_1\Delta T}{\Delta T} & \cdots & \frac{\sin v_2\Delta T(N-1) - \sin v_1\Delta T(N-1)}{\Delta T(N-1)} \\ \frac{\sin v_2\Delta T - \sin v_1\Delta T}{\Delta T} & v_2 - v_1 & \cdots & \vdots \\ \vdots & \ddots & \ddots & \frac{\sin v_2\Delta T - \sin v_1\Delta T}{\Delta T} \\ \frac{\sin v_2\Delta T(N-1) - \sin v_1\Delta T(N-1)}{\Delta T(N-1)} & \cdots & \frac{\sin v_2\Delta T - \sin v_1\Delta T}{\Delta T} & v_2 - v_1 \end{bmatrix}. \tag{13}$$

Collecting (9), (10) and (12), the cost function (4) becomes

$$\begin{aligned} \min_{R_x, R_y} J &= \min_{R_x, R_y} (w_1 J_{12} + w_2 J_{34} + w_3 J_{56}) \\ &= \min_{R_x, R_y} (-2w_1 (R_x^T M_{yx}^T R_{0x} + R_y^T M_{yy}^T R_{0y}) \\ &+ R_x^T (w_1 M_{yx}^T M_{yx} + w_2 M_{zux}^T M_{zux} + w_3 M_{zux}^T \overline{M}_e M_{zux}) R_x \\ &+ R_y^T (w_1 M_{yy}^T M_{yy} + w_2 M_{zuy}^T M_{zuy} + w_3 M_{zuy}^T \overline{M}_e M_{zuy}) R_y. \end{aligned} \tag{14}$$

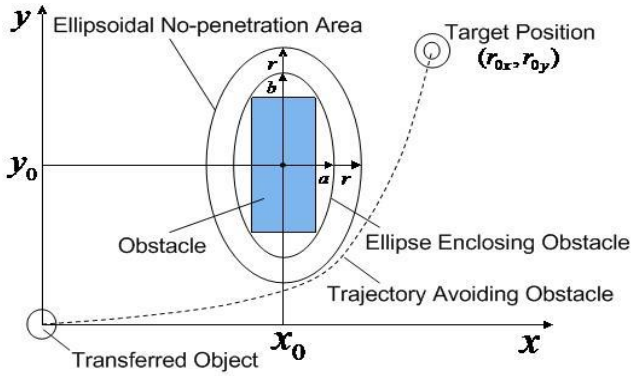


**Figure 3.** Trajectory planning with obstacle avoidance

*3.3. Input and state constraints on the transfer system*
The input and state constraints on the transfer system can be expressed into the matrix representation as

$$|M_{zxm}R_m| \leq Z_{xmc}, \quad |M_{zum}R_m| \leq Z_{umc}, \quad (m = x, y), \tag{15}$$

where $Z_{xmc}$ and $Z_{umc}$ are the input and state constraints, respectively given by

$$Z_{xmc} = \begin{bmatrix} z_{mc} & \cdots & z_{mc} \end{bmatrix}^T, \quad Z_{umc} = \begin{bmatrix} z_{umc} & \cdots & z_{umc} \end{bmatrix}^T, \quad (m = x, y), \tag{16}$$

where $z_{mc}$ and $z_{umc}$ are the boundary parameters of the constraints.

In this study, the trajectory is planned over a finite time interval. To transfer the object to the goal position ($r_{0x}$, $r_{0y}$) and ensure it is stationary at the final time, we impose the following equality constraints.

$$M_{fm}R_m = Z_{fm}, \quad (m = x, y), \tag{17}$$

where $M_{fm}$ and $Z_{fm}$ are given by

$$M_{fm} = \begin{bmatrix} C_{yclm}A_{clm}^{N-2}B_{clm} & \cdots & C_{yclm}B_{clm} & D_{yclm} \\ C_{zclm}A_{clm}^{N-2}B_{clm} & \cdots & C_{zclm}B_{clm} & D_{zclm} \end{bmatrix}, \quad Z_{fm} = \begin{bmatrix} r_{0m} \\ 0 \end{bmatrix}, \quad (m = x, y). \tag{18}$$

*3.4. Positional constraints on obstacle avoidance*
In the 2-D transfer, it is necessary to avoid obstacles in the transfer space. The obstacle is defined as the ellipsoidal no-penetration area as shown in Figure 3. The interior of the ellipse is the no-penetration area that must be avoided in trajectory planning. Therefore, we impose the following inequality constraint on the position of the transferred object.

$$\frac{(x - x_0)^2}{a_r^2} + \frac{(y - y_0)^2}{b_r^2} - 1 \geq 0, \tag{19}$$

where $(x_0, y_0)$ is the center of the ellipse. $a_r$ and $b_r$ are respectively the lengths of axes of the ellipsoidal no-penetration area, and are given as

$$a_r = a + r, \quad b_r = b + r, \tag{20}$$

where $a$ and $b$ are the corresponding axis lengths of the ellipse enclosing the obstacle. And, $r$ is represented as

$$r = r_e + d_{max}, \tag{21}$$

where $r_e$ is the radius of the circle enclosing the transferred object. $d_{max}$ is the maximum moving distance of the transferred object which is caused by leaned the rope due to inertia. The maximum rope angle $\phi_{max}$ leaned by inertia can be derived from (1) as

$$\phi_{max} = \frac{|a_x|_{max}}{g}, \tag{22}$$

where $|a_x|_{max}$ is the maximum acceleration of cart transfer. Therefore, the maximum moving distance $d_{max}$ can be represented as

$$d_{max} = \frac{l_{max}|a_x|_{max}}{g}, \tag{23}$$

where $l_{max}$ is the maximum rope length.

The matrix representation of the inequality (19) can be represented as

$$R_x^T(\frac{1}{a_r^2}M_{yx}^T E M_{yx})R_x + R_y^T(\frac{1}{b_r^2}M_{yy}^T E M_{yy})R_y - (\frac{2}{a_r^2}X_0^T E M_{yx})R_x - (\frac{2}{b_r^2}Y_0^T E M_{yy})R_y + \frac{1}{a_r^2}X_0^T E X_0 + \frac{1}{b_r^2}Y_0^T E Y_0 - \eta \geq 0 \tag{24}$$

where $E = [e_1^T e_1 \cdots e_k^T e_k \cdots e_n^T e_n]^T$, $\eta = [e_1 e_1^T \cdots e_k e_k^T \cdots e_n e_n^T]^T$, $e_1 = [1, 0, 0, 0, \cdots, 0] \in R^{1\times n}$, $e_i = [0, \cdots, 0, 1, 0, \cdots, 0] \in R^{1\times n}$, $X_0 = [x_0, x_0, \cdots, x_0]^T \in R^{1\times n}$ and $Y_0 = [y_0, y_0, \cdots, y_0]^T \in R^{1\times n}$.

By (14), (15) and (24), The trajectory planning of the overhead traveling crane can be resulted to quadratic programming problem with quadratic constraints. This quadratic programming problem is solved by a sequential quadratic programming method.

## 4. Fast solution by using feasible initial trajectory

The transfer trajectory can be obtained by the optimization problem introduced in the previous section. However, it takes a long time to derive the optimized trajectory because of many variables in the optimization. In the previous study [14], the initial trajectory $R_{ini} \in R^{1\times n}$ in the optimization has been given as

$$R_{inim} = [r_{0m}, r_{0m}, \cdots, r_{0m}], \quad (m = x, y) \tag{25}$$

where $r_{0m}$ is the target position. Thus, the initial trajectory is no-feasible solution to be subject to (15), (17) and (24). In this case, it takes a long time to obtain the optimized trajectory. By giving the feasible initial trajectory to the optimization problem, the optimizing time can be shortened. The feasible initial trajectory is designed while satisfying the constraint conditions defined by (15), (17) and (24). And, the feasible initial trajectory is designed based on the designer's subjective view.

As an example, the feasible initial trajectory is shown in Figure 4 and Figure 5. Figure 4(a) and (b) show the time series of feasible initial trajectory on $x$- and $y$-axes, respectively. Figure 5 shown the designed feasible initial trajectory on the transfer space. In the transfer space, the target position is located at $(x, y) = (1.0, 0.4)$[m]. The constraints conditions of transfer velocity, acceleration and control input are given from the specifications of the overhead traveling crane as shown in Table 1.

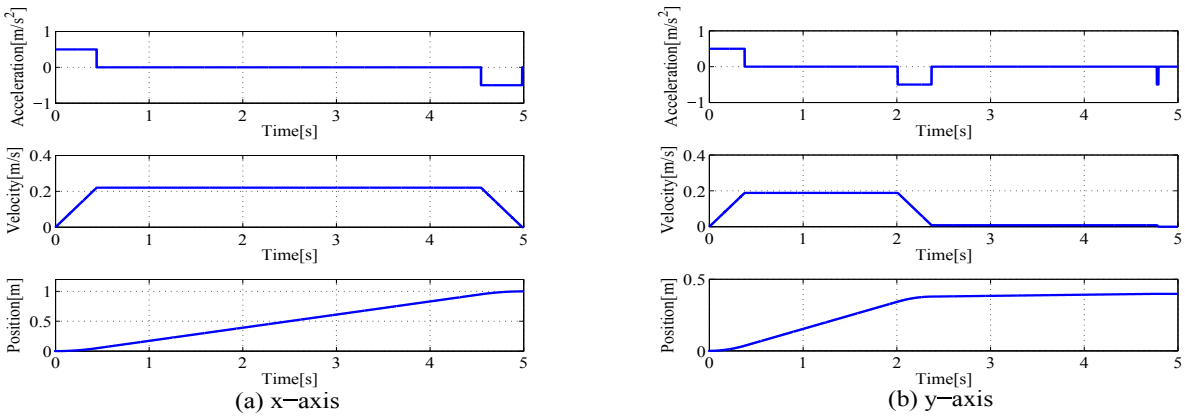


**Figure 4.** Time series of feasible initial trajectory

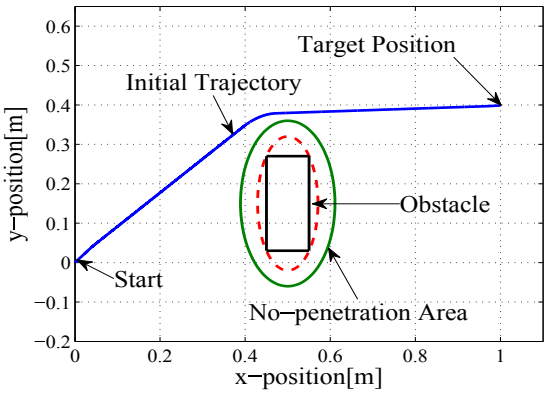


**Figure 5.** Feasible initial trajectory on transfer space

The center of obstacle is located at $(x, y) = (0.5, 0.15)$ and the size of obstacle is $H0.24 \times W0.1$[m]. Therefore, the major and minor axes of the ellipse enclosing the obstacle are $a = 0.170$[m] and $b = 0.071$[m], respectively. The maximum rope length in the overhead traveling crane is $l_{max} = 0.6$[m], and the maximum acceleration is $a_{max} = 0.5$[m/s$^2$]. Thus, the maximum moving distance by leaned the rope due to inertia is obtained as $d_{max}$=0.03[m] by (23). The radius of the circle enclosing the transfer object is $r_e$=0.01[m]. From (20) and (21), the lengths of axes of the ellipsoidal no-penetration area is obtained as $a_r$=0.210[m] and $b_r$=0.111[m].

The feasible initial trajectory shown in Figure 4 and Figure 5 is given to the trajectory optimization.

## 5. Simulation Verification

In this study, the fast solution of trajectory optimization by using the feasible initial trajectory and the cost function with the energy saving for reducing the fluctuating motion of the cart are proposed. The proposed approaches are verified by simulation of the overhead traveling crane system which has the specifications as shown in Table 1. The transfer space with obstacle is shown in Figure 5, and the feasible initial trajectory shown in Figure 5 is given to the trajectory optimization in the simulation verification. The range of the rope length while transferring the cart is between 0.3[m] and 0.6[m]. Therefore, the natural angular frequency of the load vibration is varied between 4.04[rad/s] and 5.72[rad/s]. The frequency band for vibration suppression in

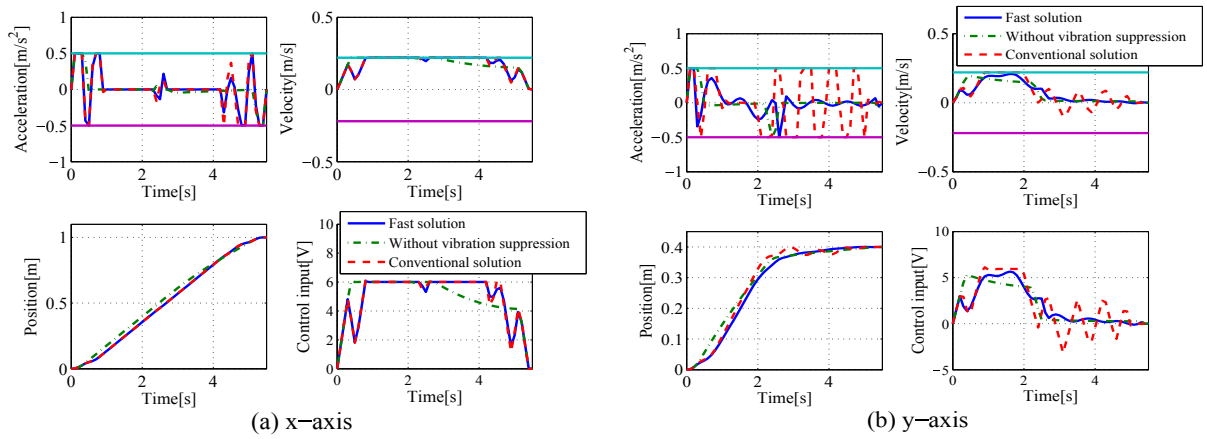


**Figure 6.** Time series in simulation results

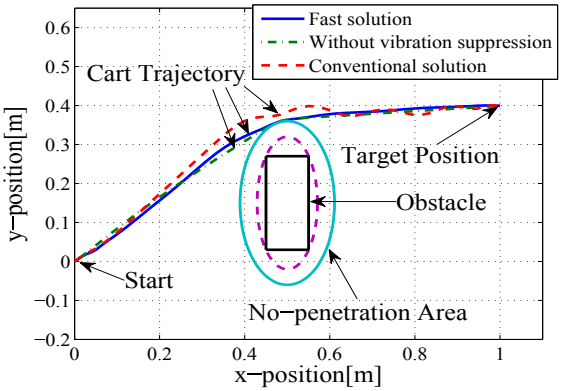


**Figure 7.** Transfer trajectory

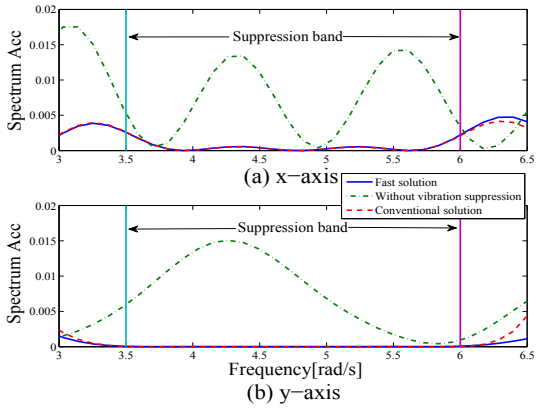


**Figure 8.** Power spectrum of acceleration of cart

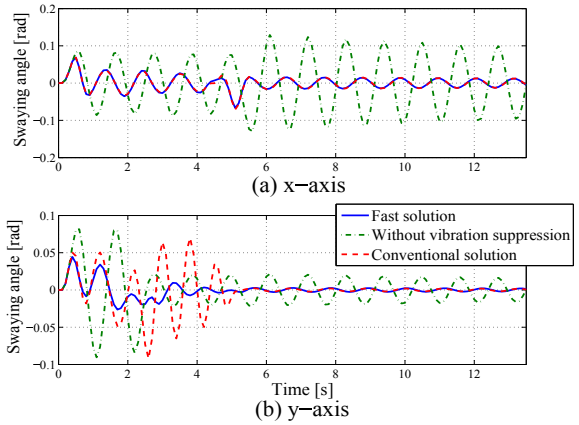


**Figure 9.** Simulation results of swaying angle, $l$=0.3[m]

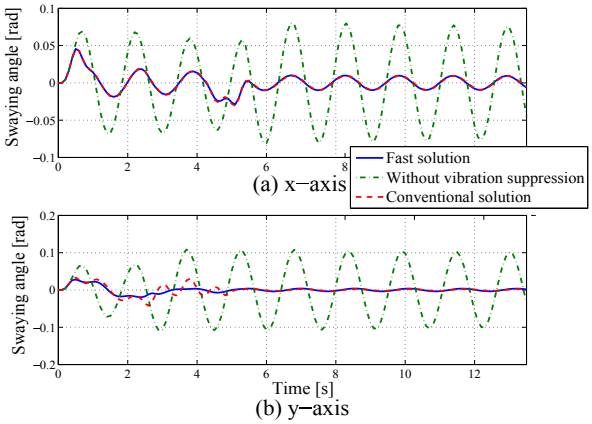


**Figure 10.** Simulation results of swaying angle, $l$=0.6[m]

**Table 2.** Optimizing time of proposed fast solution and conventional

| | Computation time [s] |
|---|---|
| Proposed solution | 111 |
| Conventional solution | 582 |

the cost function (4) is set to the range from 3.5[rad/s] to 6.0[rad/s]. The transfer time is given as 5.5[s], and the sampling time is as $\Delta T$=0.1[s].

The weight coefficients in the proposed cost function are given as $w_1$=10, $w_2$=0.1 and $w_3$=1. The trajectory optimization with the proposed cost function is performed by using the proposed fast solution. As the comparisons, the weight coefficients, which are same as the cost function in [14], are given as $w_1$=10, $w_2$=0 and $w_3$=1. And, the trajectory is optimized using the conventional initial trajectory which has the same elements as the target position $r_0$. Moreover, the trajectory is optimized using the cost function with the weight coefficients, $w_1$=10, $w_2$=0.1, $w_3$=0, which the vibration suppression is not considered in the trajectory optimization.

The simulation results are shown in Figure 6 to Figure 10. Figure 6(a) and (b) show the time series of the cart transfer on $x$- and $y$-axes in simulation, respectively. In Figure 6, the upper left graphs show the acceleration of cart transfer, and the upper right graphs show the velocity. The lower left and lower right graphs show the cart position and control input, respectively. The solid line are the simulation results of the proposed approach, the broken lines are the conventional approach and the chain lines are the trajectory without vibration suppression. Figure 7 shows the cart trajectory in the transfer space. Figure 8(a) and (b) show the power spectrum of the acceleration of the cart transfer on $x$- and $y$-axes, respectively. The line types in Figure 8 are same as those in Figure 6. Figure 9 show the swaying angle of the rope whose length is $l$=0.3[m]. Figure 10 show the swaying angle of the rope whose length is $l$=0.6[m]. In Figure 9 and Figure 10, (a) and (b) show the simulation results on $x$- and $y$-axes, respectively. The line types in Figure 9 and Figure 10 are same as those in Figure 6. As seen from these simulation results, the load swaying can be suppression by the proposed approach, and the load is transferred in a short time while avoiding the obstacle and satisfying the constraints in the crane system. Moreover, fluctuating motion of the cart can be reduced by applying the proposed cost function.

Table 2 shows the calculating time of the trajectory optimization in the proposed fast solution and the conventional solution. By using the proposed fast solution, the trajectory can be optimized in a short time.

## 6. Application to the large transfer space

The proposed approach is applied to the large transfer space. Here, the simulation conditions of the transfer trajectory are shown as follows.

· Target position is located at $(x, y) = (2.0, 0.8)$[m].

· Constraints of transfer cart are shown in the specifications in Table 1.

·The range of the rope length while transferring the cart is between 0.3[m] and 0.6[m]. Therefore, the natural angular frequency of the load vibration is varied between 4.04[rad/s] and 5.72[rad/s]. The frequency band for suppressing the vibration is set to the range between 3.5[rad/s] and 6.0[rad/s] in the trajectory planning of the cart transfer on $x$- and $y$-axes.

·The centers of obstacles are located at $(x, y) = (0.5, 0.6)$, (0.9,0.35) and (1.4,0.65). 3 obstacles has same size. Therefore, the major and minor axes of the ellipse enclosing the obstacle are $a = 0.170$[m] and $b = 0.071$[m], respectively. The maximum moving distance by leaned the rope due to inertia is obtained as $d_{max}$=0.03[m]. The radius of the circle enclosing the transfer object

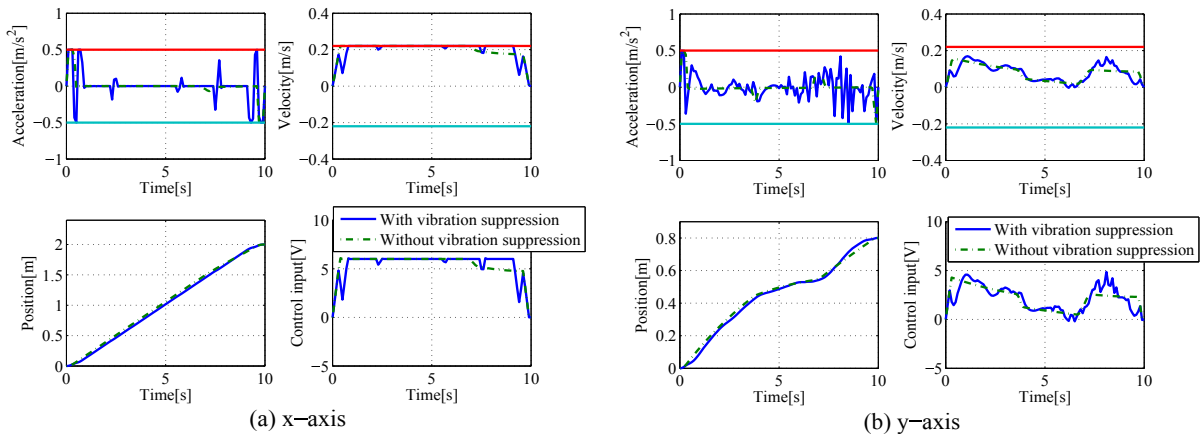


**Figure 11.** Time series in simulation results

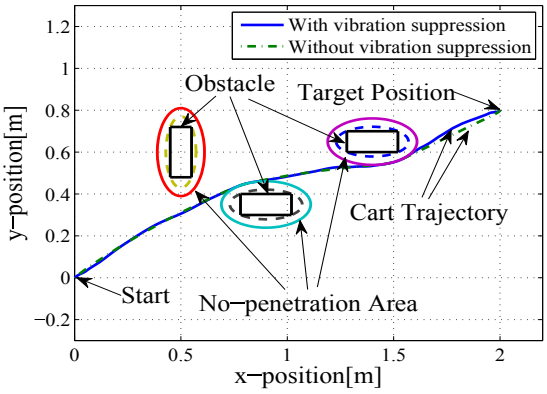


**Figure 12.** Transfer trajectory

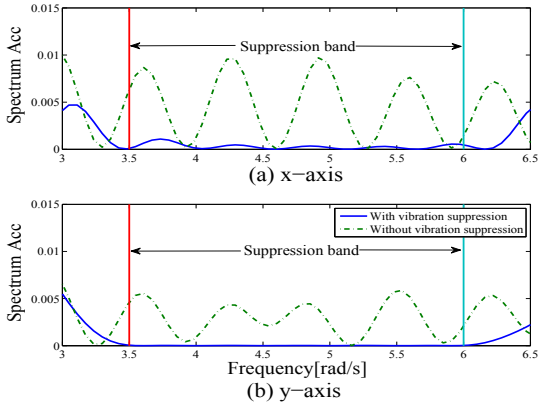


**Figure 13.** Power spectrum of acceleration of cart

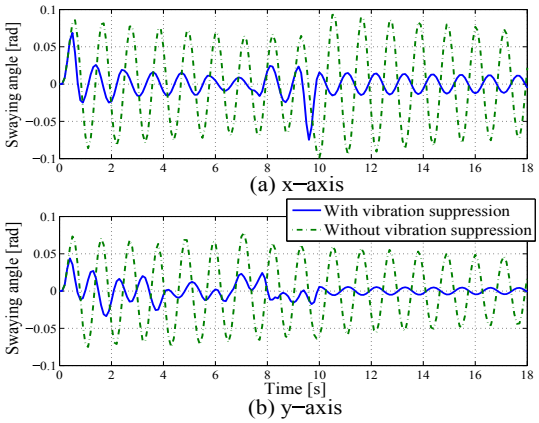


**Figure 14.** Simulation results of swaying angle, $l$=0.3[m]

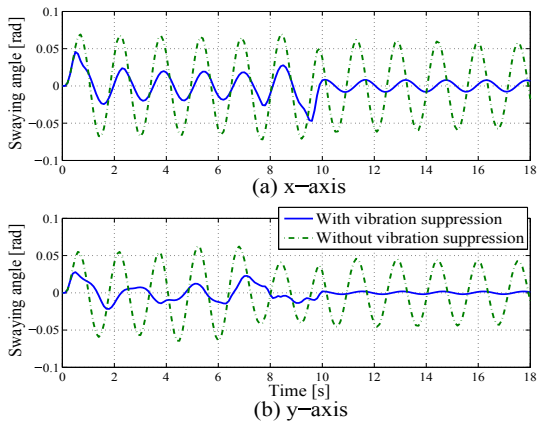


**Figure 15.** Simulation results of swaying angle, $l$= 0.6[m]

is $r_e$=0.01[m]. Therefore, the lengths of axes of the ellipsoidal no-penetration area is obtained as $a_r$=0.210[m] and $b_r$=0.111[m].

・The weight coefficients are given as $w_1 = 5$, $w_2 = 0.2$, $w_3 = 1$.

・Simulation time is given as 10.0[s] and sampling time is given as $\Delta T$=0.1[s].

The simulation results are shown in Figure 11 to Figure 15. The layouts of the figures and the line types are same as those of Figure 6 to Figure 10. As the results, the cart is transferred in a short time by the proposed approach, even if the transfer space is expanded. And, the load sway can be suppressed. The calculation time of the trajectory optimization is 2224[s]. The calculation time can be increased with expanding the transfer space.

## 7. Conclusions

We proposed transfer trajectory planning method of 2-D transfer machine with vibrational elements such as an overhead traveling crane. In this study, we especially proposed the fast solution for optimizing the transfer trajectory by giving a feasible initial trajectory. And, the cost function with energy saving was proposed for reducing the fluctuating motion of the cart. The effectiveness of the proposed transfer trajectory planning method is verified by simulations of the overhead traveling crane. The computation time of the proposed trajectory optimization is faster than that of the conventional approach. In the future works, the experimental verification using the actual crane system should be confirmed for usefulness of the proposed method, and it will be required to develop the fast solution of the trajectory optimization for large transfer space.

## 8. References

[1] Abdel-Rahman, E.M, Nayfeh, A.H, and Masoud, Z.N, 2003, Dynamics and Control of Cranes: A Review, Journal of Vibration and Control, Vol.9, pp.863-908

[2] Kawakami, S, Miyoshi, T and Terashima, K, 2003, Path Planning of Transferred Load Considering Obstacle Avoidance for Overhead Crane, *System Integration Division Annual Conference* p.640-641 (in Japanese)

[3] Yano, K, Eguchi, K and Terashima, K, Sensor-Less Sway Control of Rotary Crane Considering the Collision Avoidance to the Ground, *Transactions of the Japan Society of Mechanical Engineers*, Series(C), Vol. 68, No. 676, p.146-153, (in Japanese)

[4] Negishi, M, Masuda, H, Ohsumi, H and Tamura, Y, 2013, Evaluation of overhead crane trajectory, *JSME Conference on Robotics and Mechatronics* p.1A2-p19(1)-(4) (in Japanese)

[5] A.Z. Al-Garni, K.A.F. Moustafa and S.S.A.K. Javeed Nizami, 1995, OPTIMAL CONTROL OF OVERHEAD CRANES, *Control Eng. Practice*, Vol.3, No.9, p.1277-1284

[6] Takagi, K, and Nishimura, H, Gain-Scheduled Control of A Tower Crane Considering Varying Load-Rope Length, *Transactions of the Japan Society of Mechanical Engineers*, Series(C), Vol. 64, No. 626, p.113-120, (in Japanese)

[7] Harald, A and Dominik, S, 2009, Passivity-Based Trajectory Control of and Overhead Crane by Interconnection and Damping Assignment, *Motion and Vibration Control*, p.21-30

[8] Murakami, S and Ikeda, T, 2006, Vibration suppression for High Speed Position Control of overhead Traveling Crane by Acceleration Inputs, *Dynamics & Design Conference*, p.128(1)-(6), (in Japanese)

[9] Brunner, M, Bruggemann, B, and Schulz, D, 2012, Autonomously Traversing Obstacle: Metrics for Path Planning of Reconfigurable Robots on Rough Terrain, *Proceedings of 9th International Conference on Informatics in Control, Automation and Robotics*, p.58-69

[10] Yu-Cheng, C, Wei-Han, H, Shin-Chung, K, 2012, A fast path planning method for single and dual crane erections, *Automation in Construction*, Volume 22, p. 468-480

[11] Tamura, Y, Hamasaki, S, Yamashita, A and Asama, H, Collision Avoidance of Mobile Robot Based on Prediction of Human Movement According to Environments, *Transactions of the Japan Society of Mechanical Engineers*, Series(C), Vol. 79, No. 799, p.617-628, (in Japanese)

[12] Suzuki, M and Terashima, K, 2000, Three Dimensional Path Planning using Potential Method for Overhead Crane, Journal of Robotics Society of Japan, Vol.18, No.5, p.728-736, (in Japanese)

[13] Nakajima, J and Noda, Y, 2014, 2-D Load Transfer Control Considering Obstacle Avoidance and Vibration Suppression, *Proceedings of 11th International Conference on Informatics in Control*, Automation an Robotics, pp.653-660

[14] Noda, Y and Nakajima, J, 2015, Trajectory Planning for Vibration Suppression and Avoidance of Angularly Postured Obstacles in a 2- D Transfer System, *Mechanical Engineering Journal*, Vol. 2, No. 4, DoI : 10.1299 / mej. 15 - 00038